Annales de la Société Géologique de Belgique, T. 113 (fascicule 2) - 1990, 139-159 Février 1991

ASPECTS OF THE STRUCTURAL AND PALEOGEOTHERMAL EVOLUTION OF THE RHENISH MASSIF[1]

by

Onno ONCKEN[2]

(15 figures)

ABSTRACT.- The correlation of data on organic rank with thermally activated deformation microfabrics of frequent minerals (quartz, calcite, sheet silicates) can yield a detailed deformation-temperature history. This includes the temporal relationship of the metamorphic peak with respect to deformation, the onset and relative duration of thrust motion, the qualitative amount of thrust displacement, and the time interval of crustal stacking by thrusting, as well as of subsequent erosion.

Application of this analytical tool to published rank data from the Rhenish Massif and integration with the other fabric data mentioned show three, possibly more, regions with distinctly differing relations. Parts of the Northern Massif reach peak metamorphism during folding and cleavage formation while isolines of same organic rank are equally folded - pointing to essentially prekinematic coalification with lacking equilibration of rank to deformation conditions due to the short time available. Therefore, paleogeothermal gradients and the amount of the total sedimentary cover can be calculated from rank gradients.

In contrast, the activity of the steep to shallow dipping thrusts of the middle and southern Massif succeeds the peak of thermal metamorphism and proceeds under retrogressive conditions. This may lead to inverse rank gradients beneath the thrusts which, however, are probably not parallelled by inverse paleogeothermal gradients during thrust motion. This apparently contradictory aspect is controlled by the relative rates of thrusting, of the related motion of isothermes through the stratigraphic pile, and by the equilibration rate of the coalification reactions. The southernmost thrust system (Taunuskamm-Soonwald-thrust) moreover shows evidence of very rapid crustal stacking connected with heating of the imbricated nappe body and a following phase of rapid denudation.

1.- INTRODUCTION

In non-metamorphic or very low grade rocks which predominate in the Rhenish Massif (see Weber, 1972, 1976; Teichmüller *et al.*, 1979), petrologic data generally are not suitable - except from mafic volcanics - to determine metamorphic conditions. In these cases, a number of other parameters has been used in the Rhenish Massif which, however, do not necessarily yield the same kind of information: analysis of fluid inclusions (Koschinski 1979), data on illite crystallinity (Weber, 1972), data on organic rank (Wolf, 1972, 1978; Paproth & Wolf, 1973). The present paper makes use of thermally activated microfabrics in quartz, calcite and phyllosilicates (see Voll, 1976 and Mitra, 1987 for application in other regions) as well as of published data on organic rank which are available for most parts of the Massif.

Since some time, rank data are used to evaluate maximum temperatures during burial (Karweil, 1955, 1973; Bostick, 1973; Waples, 1980; Wood, 1988) although other authors (i.e. Tissot *et al.*, 1987) deny the possibility of determining paleotemperatures because the data rather reflect the thermal history instead of maximum temperatures. Samples from strongly folded regions with barely known burial and thermal history thus necessarily impose limitations on the deduction of metamorphic criteria from rank data. In spite of these difficulties, the reached maximum temperatures can be approximated by modelling the thermal history. In the case of reconstructable rank gradients (rank versus stratigraphic depth), data on the paleogeothermal gradients, on the amount of subsidence, and on the thermal and burial history can be computed under certain conditions (Buntebarth, 1979; Oncken, 1984, 1987). Moreover, the relationship of the rank or of lines of equal rank to a folded and stacked stratigraphic sequence allows

1.- Paper delivered at the symposium «Tectonics of the Rhenish Massif» (Ardenne and Rheinisches Schiefergebirge), organized by the Société géologique de Belgique on November 4, 1988. (Organizers: J. Bellière and D. Laduron). Manuscript received in February 1989

2.- Geologisch-Paläontologisches Institut, J.W. Goethe-Universität, Senckenberg-Anlage 32-34, 6000 Frankfurt 1, Federal Republic of Germany.

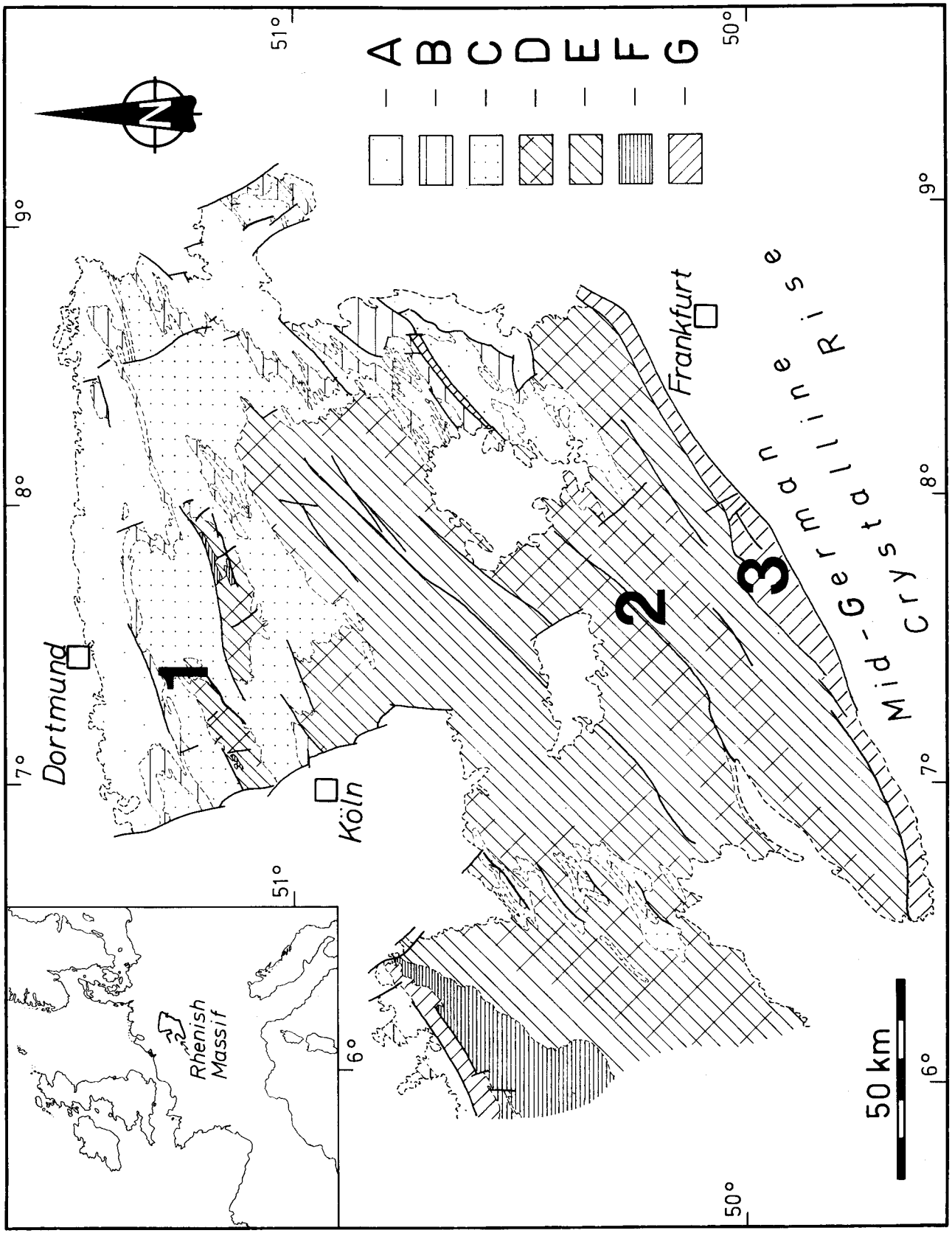

Fig. 1.- Geological map of the Rhenish Massif: A: Carboniferous; B: Upper Devonian; C: Middle Devonian; D: Emsian; E: Siegenian and Gedinnian; F: Pre-Devonian; G: undifferentiated Devonian. Numbers refer to the three regions discussed in the paper.

the reconstruction of the relative timing of peak metamorphism, folding, and thrusting. These data, when combined with deformation textures whose temporal relation to deformation history is generally well known, will even yield a still more detailed temporal resolution of the deformation-temperature history.

The aim of the present paper is to show the possible advantage of the combined use of rank and microfabric data and their application to the Rhenish Massif. Three areas along a cross section of the Massif from the northern, central, and southern Massif (see Fig.1) will be analysed by the mentioned method which is presented in more detail. Apart from the possible statements mentioned above a further key question focusses on the problem whether a significant difference can be stated between the northern and the southern Massif with respect to the thermal and structural evolution (similar to the well known difference in structural style, see Meyer & Stets, 1980; Weber & Behr, 1983).

2.- THEORETICAL ASPECTS

2.1.- Coalification and temperature

The process of coalification essentially involves the thermally induced chemical decomposition of organic matter through loss of volatile elements. The factors temperature and time practically exclusively control the reaction; chemical factors, like the presence of elements or phases with catalytic influence, or other physical factors, like confining pressure or shear stress, can be neglected since their influence is restricted to the influence on changes of the fabric - i.e. by rotation of the aromate lamellae in positions favourable for reaction (cf. Karweil, 1955; Stach, 1975; Teichmüller, 1987) - or on changes of the permeability - which may control the removal or the concentration of the decomposition products. The process of coalification as a first order reaction is described by the Arrhenius-equation

$$k = A * \exp(-E_A/RT)$$

(see Karweil 1955, Buntebarth 1979, Wood 1988 for more details) where E_A is the activation energy, R is the universal gas constant, k is the reaction constant, and A is the so-called frequency factor. The reaction constant k (in a^{-1}) represents the constant fraction of the reactants of a given untransformed group which will react per time unit (irrespective of the concentration). In the case of first order reactions, the frequency factor A (in a^{-1}) reflects the fraction of the reactants present per time unit which show the specific internal distribution of free energy capable of breaking weak bonds. The activation energy E_A (in kJ/mol) expresses the total energy of a molecule needed to break weak bonds with a favourable distribution of free energy. The exponential term thus describes the temperature-dependant fraction of the reactants whose energy is large enough to lead to decomposition under favourable conditions (see above).

The activation energy as well as the frequency factor of coalification reactions are only known approximately. Most authors presume that the activation energy is not a constant, since the relative share of the participating reactions depends on the temperatures and the changing reaction products during coalification (e.g. Karweil, 1973; Tissot *et al.*, 1987; Wood, 1988). Similar aspects concern the frequency factor. Because of the different reactants participating in the reactions, a set of kinetic parameters which would depend on the composition of the organic matter and its change during organic metamorphism should be available (these aspects are taken account of by Bostick *et al.*, 1979 and Wood, 1988).

On the basis of the analysis of paleozoic coals from the Ruhr district, Karweil (1973) determines an activation energy of 35.2 kJ/mol for petroleum generation, Tissot *et al.* (1987) give values of 220-230 kJ/mol for young coals (type II kerogene, cf. Wood, 1988).

On the basis of the analysis of paleozoic coals from the Ruhr district, Karweil (1973) determines an activation energy of 35.2 kJ/mol, Hood *et al.* (1975) mention 83-125 kJ/mol for petroleum generation, Tissot *et al.* (1987) give values of 220-230 kJ/mol for young coals (type II kerogene, cf. Wood, 1988). The present paper makes use of the data of Karweil (1955, 1973) and their supplementation by Bostick (1973) as well as of the data of Bostick *et al.* (1979) while using the maximum vitrinite reflection as rank parameter (see Teichmüller 1987 on problems with this parameter). The generally used graph of the Arrhenius equation as the logarithm of the reaction constant versus the reciprocal absolute temperature (in °K) gives a number of straight lines for different rank stages (see Fig.2).

The Figure does not show the reaction curves which may be derived from the data of Wood (1988). The effect of higher activation energies (as compared to the Karweil data) is expressed by a markedly lower time dependance of the reaction (= *steeper slope of the curves). At times of effective coalification (see below for definition) between 10-30 Ma the results computed from the different kinetic parameters approximately coincide with each other; Karweil's diagramm will predict higher temperatures at shorter times and*

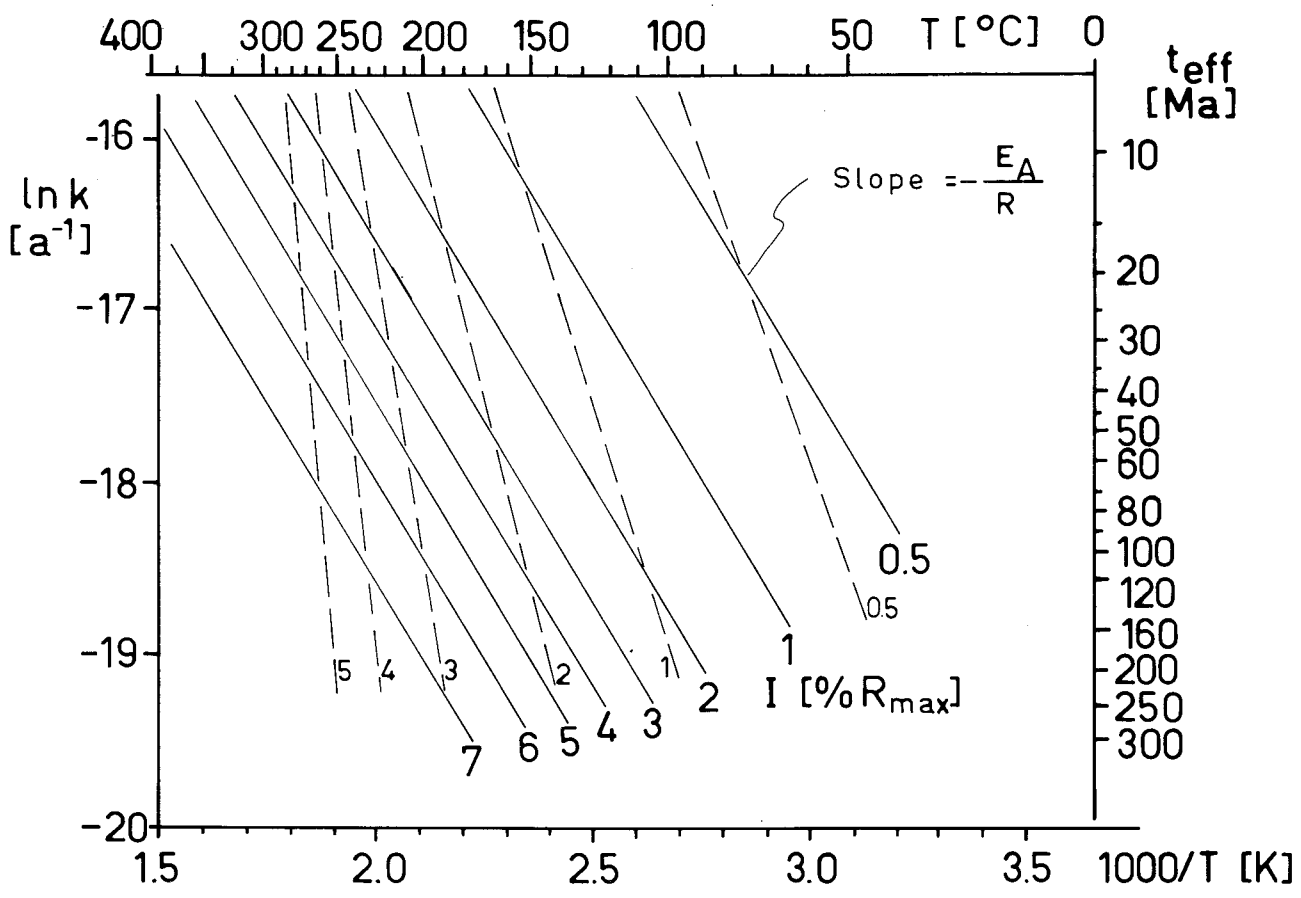

Fig.2.- Arrhenius-diagram of the coalification reaction (with %R_{max} of vitrinite as rank parameter) showing dependence on temperature and effective time of coalification; solid lines: from data by Karweil (1973) and Bostick (1973); dashed lines: reaction curves from data of Bostick *et al.* (1979), in this case the effective time of coalification follows the definition of Hood *et al.* (1975): the time the specimen has spend within 15°C of the maximum temperature; see text for different usage of the term.

lower temperatures at longer time intervals as compared to the data of Bostick et al. (1979) and Wood (1988).

2.2.- Coalification and time

The organic particles are not effected by the peak temperatures reached from the start of sedimentation, and the reaction may still proceed somewhat during decreasing temperatures. Because of these aspects and of the time dependance of the coalification reaction, the time of coalification must take into account the changing temperatures as well as the delay of equilibration to the prevailing temperature. This effect is described by the «effective time of coalification» which is defined differently from Hood *et al.* (1975) as the time necessary to transform the entire amount of vitrinite at constant temperatures to a specified rank. Similar to Bostick's solution (1973), the true time of coalification (t) is multiplied with ,the quotient of the integral of the temperature history and the product time* temperature (also see Buntebarth, 1979) $t_{eff} = x*t$, where the true and the effective time of coalification are given in million years. The quotient x thus becomes

$$x = (T * t)^{-1} * \int_{t=o}^{t=ti} T(t)\, dt$$

This representation practically expresses the amount of heat (energy) required for a specific degree of transformation (rank). At approximately stable paleogeothermal gradients during burial, the integral of temperature history - which in general is not well known - can be substituted by the integral of the subsidence history (see Fig.3, with depth of burial z given in km). The depth of burial recorded along the abscissa of a time-burial diagram thus represents a specific temperature and geothermal gradient. In no case should it be mistaken to be equivalent to a conventional depth of burial (or confining pressure): temporal changes of the gradient are possible; moreover, a particle will generally go through the peak temperature during beginning uplift due to a loop-like PT-path. This latter time interval however is shown in the diagram as the apparent maximum depth of burial.

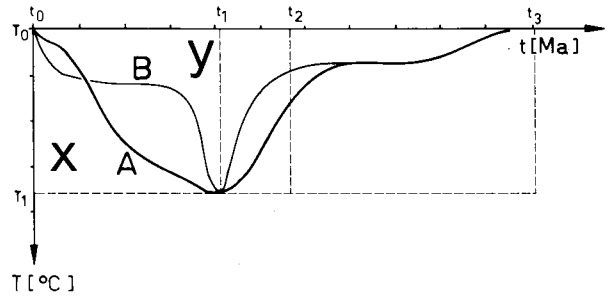

Fig. 3.- Characteristic time-temperature curves (or time-burial curves at linear, constant geothermal gradients); A for simple subsidence and uplift, B showing the form of the curve for a period of tectonic stacking and erosion following basin subsidence. The integral of the thermal history is determined from the areal quotient y/(x+y); the effective time of coalification is independent from the choice of the lower time limit of coalification (t_1, t_2, t_3 in the diagram) as long as the chosen time covers the period until the thermal peak («maximum burial»); the examples A and B shown have different times of effective coalification and therefore should exhibit - in spite of the same temperatures reached - different organic rank.

The procedure may be accomodated to the more general case with varying geothermal gradients by a simple modification: Instead of a linear scale for the depth of burial paralleling the linear temperature scale, the abscissa is divided into seperate depth-scales for every section of the history related to a different paleogeothermal gradient. The time-tmeperature curve may then be redrawn with a linear scale of depth; this correct time-burial diagram however can not be used to determine the effective time of coalification. Data on depth of burial are usually derived from subsidence curves, rank profiles (see Oncken 1984, 1987), or other sources; the time of burial can only be approximated from data on stratigraphy, from the development and the end of sedimentation, and from erosion history.

For a number of cases, an unequivocal rank gradient (rank versus stratigraphic depth) can not be reconstructed; also, data on sedimentation history may be scarce. Thus, a direct evaluation of paleotemperatures may not be possible, since the effective time of coalification can not be determined. However, the analytic tool presented may yield other valuable information under certain conditions: If the peak temperature reached is known from other sources (petrologic data, fluid inclusion data, etc.), Fig.2 may be used to give the effective time of coalification for given rank data. The effective time of coalification is then used to calculate the variable x from the equally known total time of coalification (which should be chosen to at least cover the time span from the start of sedimentation to the peak temperature or final depth). The data on subsidence and erosion history, as well as on the time of peak metamorphism can now be compiled to reconstruct the outlines of the time-temperature curve (Fig.3). This curve is then converted to a time burial curve while taking in account a set of paleogeothermal gradients for the different segments of the burial history. The temperatures derived from petrologic criteria thus essentially should be able to «explain» the rank observed. The degree of confidence obtained from the reconstruction of the temperature history of a particle increases - the «explanation» of the observed rank is corroborated -, if the rank of different neighbouring stratigraphic levels are incorporated: The burial model has to be able to explain common aspects as well as differences of this local group of rank data from the temperature history.

2.3.- Concluding remarks

Since the values for the kinetic parameters for coals of different composition, rank, and stratigraphic age are not known sufficiently well at present, an inevitable uncertainty is imposed on the exact reconstruction of paleotemperatures. Moreover, the determination of vitrinite reflectance may be subjected to some error resulting in scatter (see Wolf, 1972; Stach *et al.*, 1975; Tissot *et al.*, 1987). Taking in account the estimated error for t_{eff} of $< 20\%$, the degree of confidence for the reconstruction of paleotemperatures can be assessed: The possible deviation in the range of reflectance (%R_{max}) from 2-8 and from 20-80 Ma (t_{eff}) is +/- 20°C for the set of kinetic parameters used in Fig.2. At effective times of coalification exceeding 40 Ma or remaining below 10 Ma, the possible error may rise significantly: from +15% to -25% (depending on the values for the activation energy and the frequency factor).

The available data on rank (sources will be listed) and coalification gradients (see Oncken, 1984) thus yield suitable information to evaluate the order of magnitude of the paleotemperatures and the depth of burial. However, the time of maximum temperatures and of greatest depth of burial can not be taken to exactly coincide. Rather, a loop-like PT-path during subsidence followed by uplift will have the consequence of a delay of the peak temperatures behind the time span of maximum burial. The relationship of this evolution to the time interval of deformation is generally shown by the relationship of the lines of equal rank to the deformed stratigraphic sequence. The relative timing of peak metamorphism, maximum burial and deformation are thus easily obtained.

3.- ORGANIC METAMORPHISM, MICROFABRICS, AND MINERALISATION

A number of papers focussing especially on the Swiss Alps has established the relationships between diagnostic minerals or mineral assemblages to organic rank in order to differentiate between metamorphic levels in very low grade and low grade rocks (e.g. Frey & Niggli, 1971; Kübler *et al.*, 1979; Frey *et al.*, 1980; Kisch, 1980; Breitschmid, 1982; Frey, 1987). In addition, several authors have attempted to construct a common metamorphic scale from the correlation of rank data and illite crystallinity (e.g. Frey & Niggli, 1971; Wolf, 1975; Teichmüller *et al.*, 1979; Frey *et al.*, 1980; Kisch, 1980; Frey, 1987; Teichmüller, 1987). The results of the cited papers are not in general agreement showing special relationships for different regions, and giving only a general trend. The comparability is essentially affected by the different kind of information reflected: The parameters relevant for the Arrhenius equation of a chemical reaction (t, T) on one side, and the additional effects of strain (free strain energy, grain boundary energy), of grain size, and of the chemical environment on the other side.

In addition to the mentioned relationships between different metamorphic indicators, the present paper uses the sum of observations (from the Rhenish Massif!) on deformation fabrics within abundant minerals (quartz, calcite, phyllosilicates) and the appearance of several mineralisations; the relationship of these fabrics to the temperatures reached is estimated from neighbouring rank data. Because of the time-dependance of the coalification reaction, rank data may only be used as temperature indicators, if a correction of the time aspect has been carried out. A suitable parameter proposed here is the normalised rank I_N calculated on the basis of Karweil's (1973) data (also see Fig.4):

$$I_N = I/(t_{eff})^{1/3}.$$

This parameter can be applied to the cases with effective time of coalification between 20 and 200 Ma (at shorter times, the same value for I_N will give higher temperatures). The simple, nearly linear relationship of this parameter to temperature is illustrated in Fig.4. A similar relationship with the data of Bostick *et al.*, 1979 is achieved with $I_N = I/(t_{eff})^{1/4}$. Since this parameter permits a less ambiguous correlation to other metamorphic criteria of this grade, metamorphic levels (diagenesis - very low grade - low grade) are

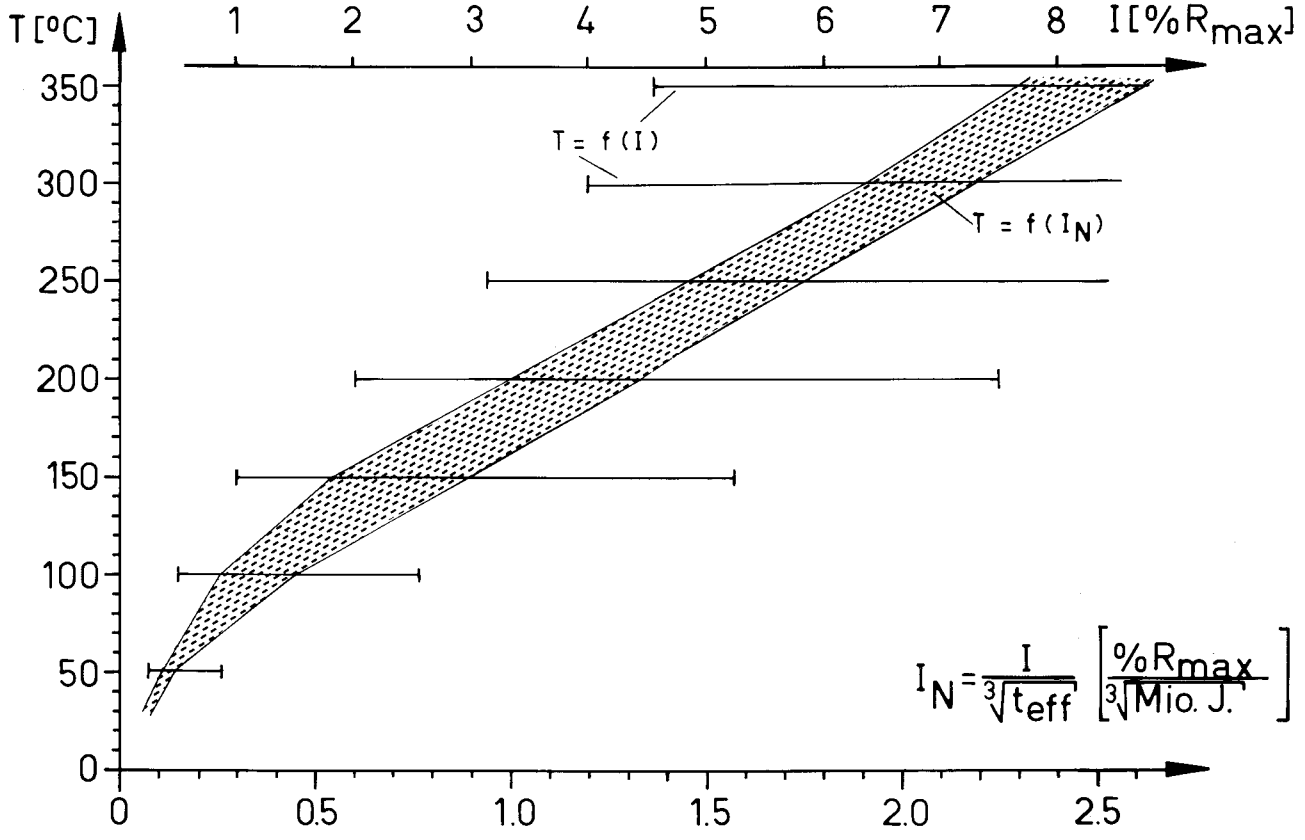

Fig.4.- Relationship of rank (maximum vitrinite reflectance I) and normalised rank (I_N) to temperature for effective times of coalification from 20 to 200 Ma on the base of the data from Karweil (1973).

differentiated more easily. The use of the reflectance of vitrinite, often used to this effect besides illite crystallinity, has the unsatisfactory consequence of stating metamorphic boundaries as a function of time - they will thus be placed differently in regions with different time-temperature history and approximation to equilibrium. Generally however, this aspect is equally valid for other metamorphic reactions and for the thermally activated motion of dislocations during recovery processes; their kinetics are also described by an Arrhenius-type equation (see Nicolas & Poirier, 1976; Vernon, 1983). In this case, the number of the necessary geometrical and physical variables is considerably larger however. The driving force during motion of grain boundaries (product of dislocation density and dislocation energy) for example, as part of the frequency factor, is strain dependant (increasing dislocation density and/or heating time lower the temperature necessary for recovery processes to a lower temperature limit). The large number of variables generally limits the possibilities to normalise to time like in the case of rank data.

These considerations illustrate that the different directly observable parameters are generally incommensurable. The attempt of a correlation of different criteria is undertaken in spite of this problem and relies on the condition that no equilibrium states are analysed and compared: Due to continuous progressive deformation under changing conditions, the fabrics used will not reflect a state of equilibrium of the rock to specific PT-conditions (as well as to chemical environment and P_{fluid}). Figure 5 thus only registers the first microscopically evident appearance of a fabric type (or mineral) in the usually rather heterogeneously deformed specimens (cf. similar diagrams from Kübler *et al.*, 1979; Breitschmid, 1982). Heating time and reaction constants thus

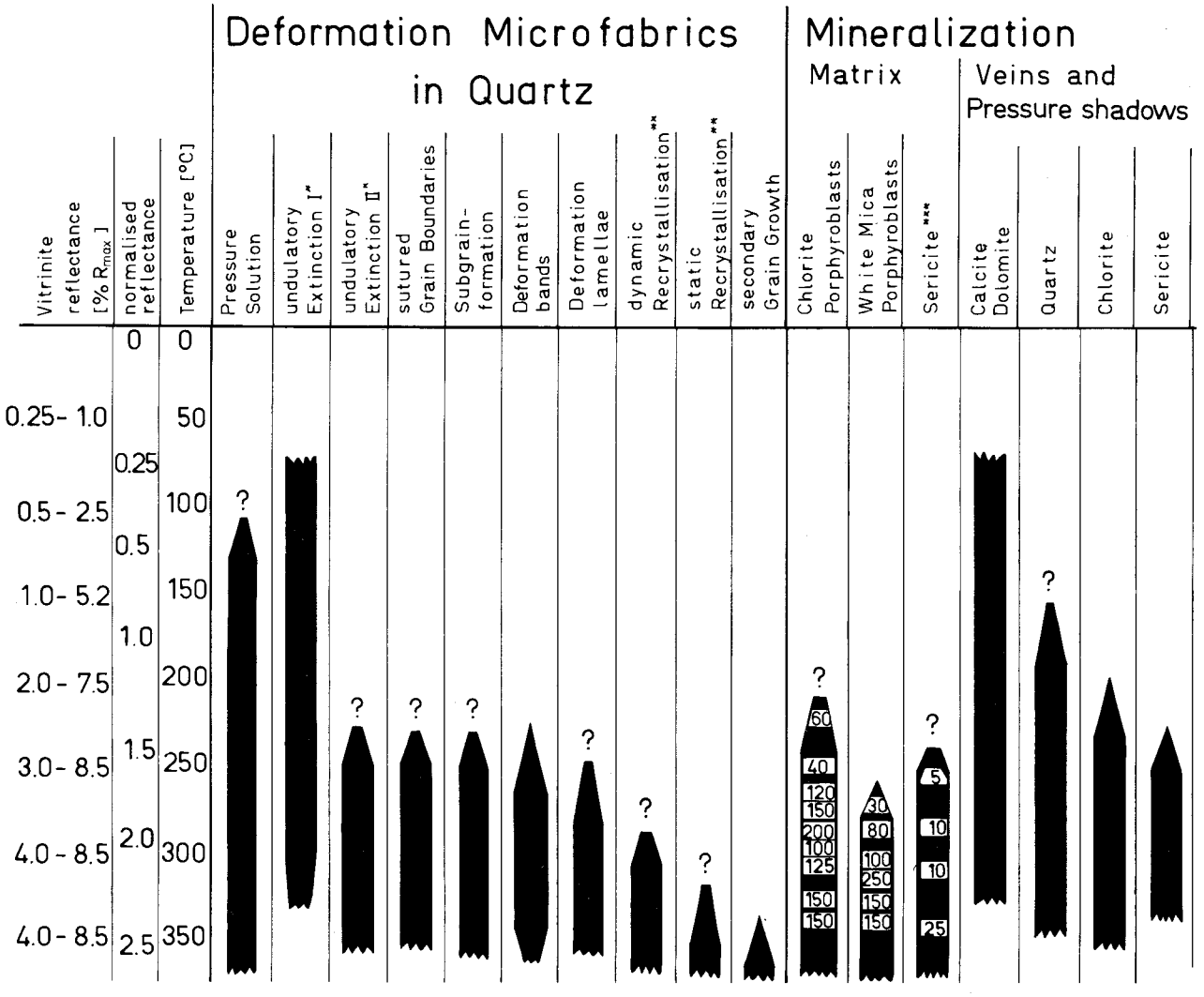

Fig.5.- Occurence of deformation fabric types in quartz and of mineralisations depending on temperature. *: I=continuous, II=discontinuous undulatory extinction; **: differentiated by formation ofstraight equilibrium grain boundaries, grain shape, and pattern of crystallographic orientation; ***: white mica with undetermined composition; numbers in matrix mineralisations give observed grain sizes in μm.

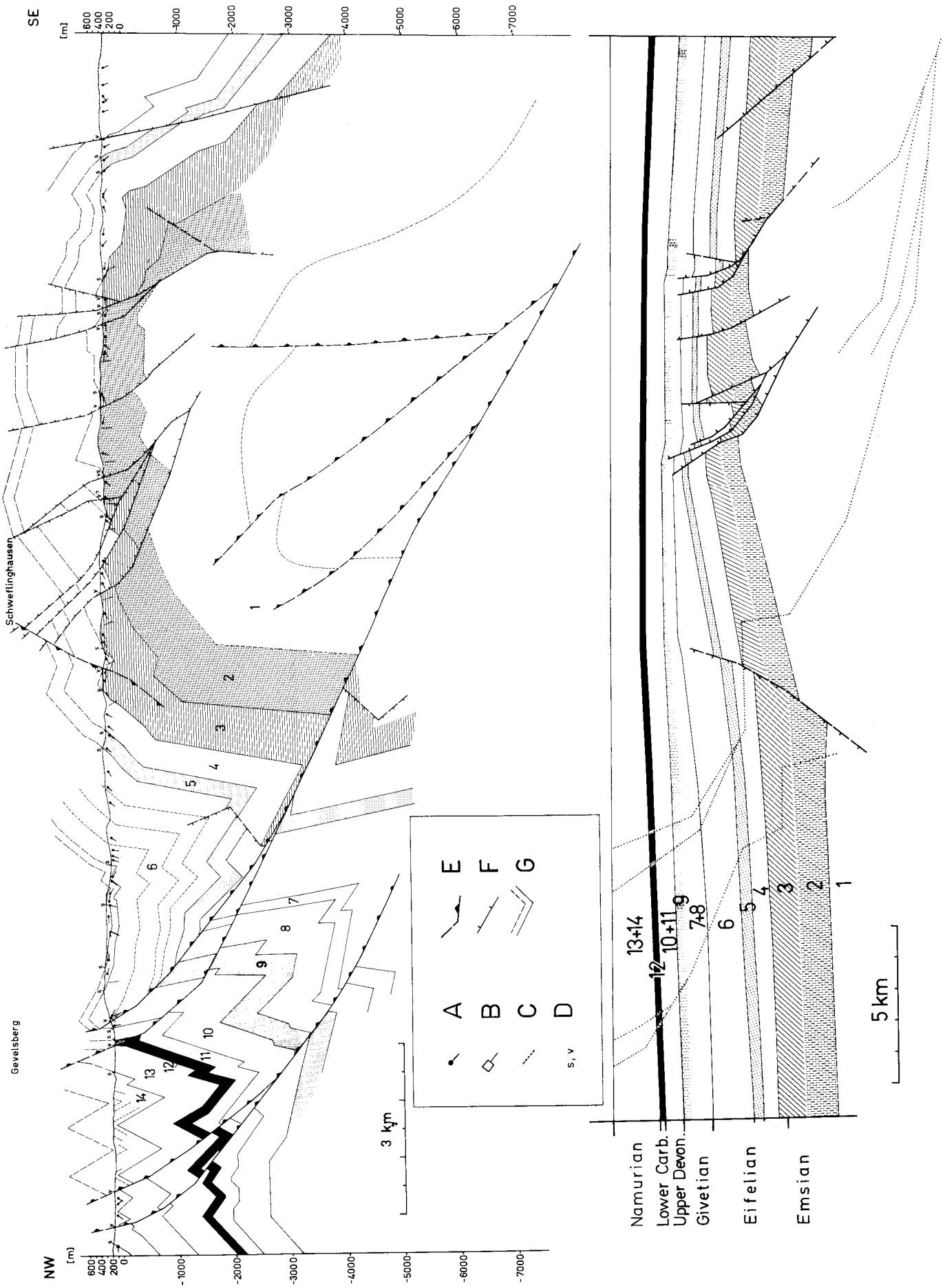

Fig.6.- Balanced cross section and restored section across the Remscheid anticline and the Ennepe reverse fault; A: apparent dip of bedding; B: apparent dip of enveloping plane of minor folds; C: apparent dip of (first, i.e. dominating) cleavage; D: mapped stratigraphic boundaries (s) and faults (v); E: reverse fault, thrust (when dashed showing assumed position); F: normal fault; G: stratigraphic boundary in section (dashed: bedding planes used to support construction).

do not play any significant role as long as only the lower temperature threshold for the first appearance on a microscopic level is regarded.

A further essential condition for the calibration of fabric types to temperature is a comparable, high strain (because of the contribution of the strain energy to the activation energy) which must have been reached before or during peak temperatures. To fulfill this condition, only regions with high strains ($R_{xz} > 2.0$) are considered. Quartz fabrics are moreover analysed only from large grains (> 100 μm) in pre- to syn-S_1-veins and are not taken from the smaller, often matrix-supported detrital grains which preferentially deform by other mechanisms (i.e. pressure solution). This procedure guarantees the obtaining of data which pertain to the thermal peak - generally synkinematic to S_1 in the Rhenish Massif (see Weber, 1972, 1976; Ahrendt *et al.*, 1978; Oncken, 1988) - and more reliably reflect the lower temperature limit of recovery processes - generally observed to be induced more easily in large grains (White, 1976; Nicolas & Poirier, 1976). Because of the large amount of fluid inclusions (dispersed diffusely as well as concentrated along syntaxial microcracks), the recovery processes are moreover thought to proceed in a hydrolytically weakened lattice (see White, 1976 and Nicolas & Poirier on this aspect) thus retaining the lowest possible temperatures at the strain recorded.

The discussion of the subsequently presented temperature relations must however take into consideration that the basic correlation between temperature and rank used here is subject to several uncertainties (see above) which allow only the calculation of approximate figures. A number of essential relationships are obtained: The lower temperature threshold calculated for dynamic recrystallisation of quartz agrees well with data by Voll (1976) deduced from petrological observations (ca. 275°C); static annealing with formation of equilibrated high angle grain boundaries (120° triple points) and subsequent secondary recrystallisation (grain growth) appear to start at only slightly higher temperatures; recovery fabrics in quartz (sutured grain boundaries, subgrains and discontinuous undulatory extinction, deformation bands and lamellae) appear between 200 and 250°C; microscopic evidence for pressure solution of quartz seems to occur somewhat earlier than the formation of quartz in veins and pressure shadows at temperatures around 100° (cf. similar values from Kerrich *et al.*, 1977). Although much less observations are available on calcite, the analogous fabric types seem to occur at roughly the same conditions as for quartz - possibly shifted to somewhat lower temperatures. The threshold for polygonisation of sheet silicates in the cleavage microlithons approximately agrees with the onset of quartz recrystallisation (comp. Weber, 1976).

Chlorite porphyroblasts (as «cross mica» on detrital muscovite or quartz) and chlorite in veins and pressure shadows appear simultaneously at roughly 200° (see also sericite). Generally, these observations relate to Fe-rich chlorites (cf. Weber, 1976; White & Knipe, 1978; Knipe, 1981). The formation of white mica porphyroblasts throughout starts at higher temperatures. Generally, the appearance of both types of porphyroblasts is constricted to highly strained areas with penetrative cleavage - they thus also seem to belong to the group of strain-dependant fabrics. This is also supported by investigations on strain-dependant metamorphism during cleavage in pelitic rocks (see Knipe, 1981). The appearance of albite in veins is simultaneous to the appearance of chlorite, apatite follows at somewhat higher temperatures.

The mentioned relationships pertain essentially to the Rhenish Massif with its specific time-temperature history and deformation conditions. On the whole, however, the boundary between diagenesis and very low grade metamorphism usually placed at some 200°C (see Teichmüller *et al.*, 1979; Winkler, 1979; Breitschmid, 1982) also seems to be the relevant limit with respect to the occurence of the fabric types and minerals investigated here. The subsequent stage of meta-anthracite thus also characterises a change in reaction to deformation of the essential rock-forming minerals in the sense of an increasing role of work-softening processes controlled by crystal-plastic and diffusion-controlled mechanisms.

4.- REGIONAL STRUCTURE AND PALEOGEOTHERMICS

4.1.- The northern Massif

The structure of the northern Rhenish Massif is characterised by large, upright, and weakly NW-vergent anticlines and synclines (10-30 km fold length) often related to large reverse faults on the northern flanks of the anticlines (see Remscheid, Fig.6, and Ebbe anticline). The relatively weakly deformed structure shows a rank pattern which is specific for this part of the Massif (see Wolf, 1972; Paproth & Wolf, 1973): The anticlinal cores with Ordovician to Lower Devonian rocks show higher ranks with 5 to 8% R_{max} (260-320°C) than the neighbouring synclines (Middle Devonian to Lower Carboniferous with 2-5% R_{max}, corresponding to 220-260°C in Mid-Devonian rocks and 180-240°C in the younger footwalls of the thrusts). However, the organic metamorphism

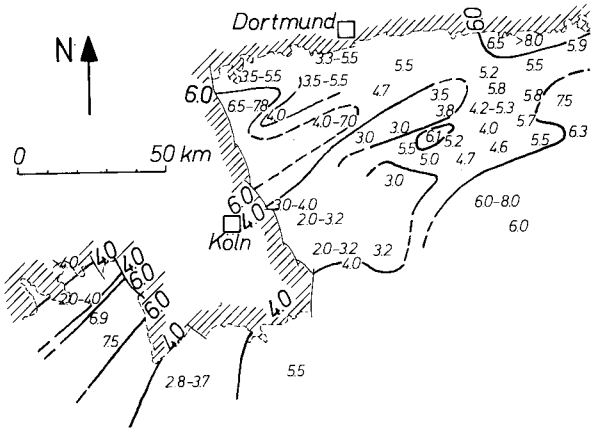

Fig.7.- Paleogeothermal gradients in the northern Massif and the Eifel (in °C/100m) as determined from rank gradients (see Oncken, 1984, 1987 for details). Thick lines give lines of equal paleogeothermal gradients; compare to large scale structures in Fig.1.

within a stratigraphic level increases in direction of the syncline. Across the reverse faults on the northern flanks of the anticlines, a considerable hiatus of rank (1-3%) can be observed; no such discontinuity is observed across the faults on the southern flanks of the anticlines: Strata of different age have the same rank here, these latter fault structures which mostly trend obliquely to the fold trend show a down-dip displacement of the hangingwall and aparently are pre-metamorphic (i.e. syn-sedimentary).

These observations are generally interpreted to reflect largely prekinematic coalification in this part of the Massif (Wolf, 1972; Paproth & Wolf, 1973; Teichmüller *et al.*, 1979; Oncken, 1984) although petrographic data point to synkinematic peak temperatures. Several features may only be observed in the anticlinal cores and the hangingwalls of the large thrusts with exception of the cooler hangingwall of the Ennepe-fault (northern flank of Remscheid anticline): Chlorite and cross mica blasts grow synkinematically to the cleavage - sometimes with pyrophyllite (Ebbe anticline); sheet silicates may start to polygonise (at $R_{max}>$ 7%) during S_1; quartz in pre- and syn-S_1-veins exhibits recovery fabrics (discontinuous undulatory extinction, formation fo subgrain boundaries), in places even the beginning of dynamic recrystallisation without however reaching equilibrated grain boundaries; K/Ar- ages of illites recrystallised during S_1 show Upper Carboniferous ages interpreted as synkinematic peak temperatures (see Ahrendt *et al.*, 1978; see also Weber, 1972, 1976; Oncken, 1988). The northern Remscheid anticline (5% R_{max}), and especially the footwalls of the Ennepe and Ebbe reverse faults (< 4% R_{max}) display none of these features; sheet silicates and quartz only show cold working (undulatory extinction, microcracks, kinking).

Due to the effect of largely prekinematic metamorphism of the organic matter, a previous paper (Oncken, 1984, 1987) was able to establish a reltionship between rank gradients (rank versus stratigraphic depth) and paleogeothermal gradients including the consideration of the effective time of coalification. Since the rank isolines in this part of the Massif are folded along with the strata, rank gradients can be used to yield the pattern of pre-orogenic heat flow. This pattern shows a strong relationship between anticlines, reduced subsidence (from thickness analysis), and elevated heat flow on one side and synclines with stronger subsidence and smaller heat flow on the other side (cf. Fig.1 and Fig.7). The interpretation of this picture must however consider an essential aspect: During folding and thrusting, the rising anticline in the thrust hangingwall will start to erode and cool, while the syncline in the footwall will subside during synorogenic stacking and receive, moreover, part of the anticlinal detritus. The gradients in the anticlines will thus reflect a truly pre-orogenic stage of paleo-heat flow, while the pre-orogenic rank differences in the synclines are overprinted slightly during folding (i.e. obliterated) and thus necessarily give lower paleogeothermal gradients (see Fig.6). On the other hand, there also seem to be primary differences in paleo-heat flow resulting from differential subsidence and other effects (Oncken, 1987; see also lack of rank difference across large pre-kinematic normal faults).

On the whole, the temperature history can only be reconstructed by taking into account several features. A high and differentiated pre-orogenic heat flow is responsible for most of the organic metamorphism in this part of the belt. Peak temperatures are reached during deformation (with formation of the recorded mineral fabrics) but are short-lived: Rank does not seem to have equilibrated entirely with synkinematic temperatures, most of the deformation must have occured rapidly under retrogressive conditions thus retaining a partly pre-orogenic paleogeothermal picture. The structural picture characteristic of parts of the northern Massif thus consists of a stretched basin filling (originally evolved on rifted and hot continental crust) with a horst and graben geometry which is overprinted by folding and thrusting (Fig.6). The resulting large scale structures partly reflect this former rift-structure and form during and after peak temperatures with a different development of anticlines and synclines.

4.2.- The Boppard Thrust

In contrast to the northern Massif, the structure of the central and southern parts of the Massif is dominated by penetrative cleavage and

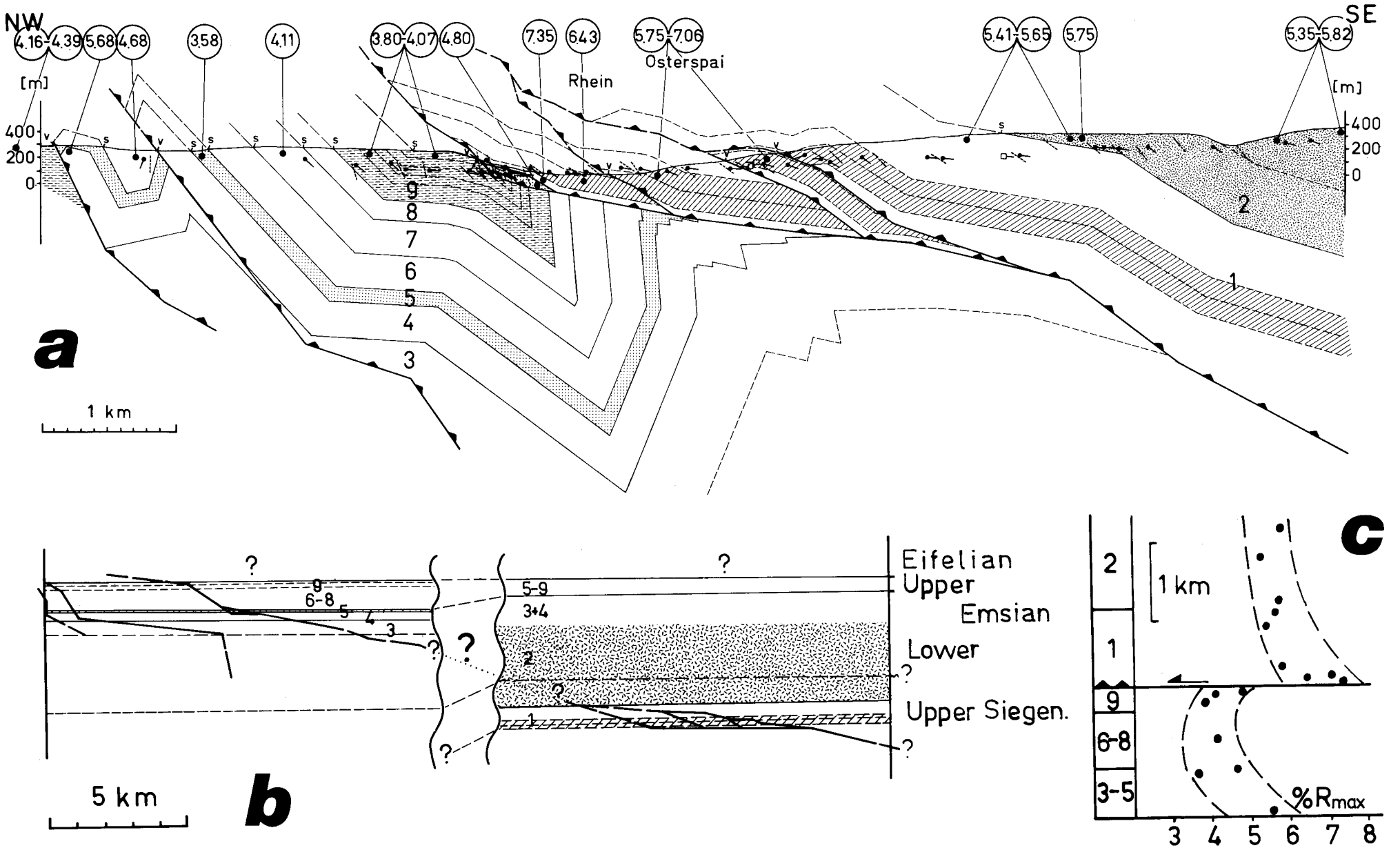

Fig.8.- Balanced cross section (a), restored section (b), and synthetic vertical rank profile (c) across the Boppard thrust along the river Rhine; the neighbouring rank data from Wolf (1978) are projected along strike above the section (in vitrinite reflectance); see Fig.6 for explanation of symbols in the section.

small to large scale imbricating of the Devonian sequence. A further characteristic feature is a succession of vergency fans which are geometrically and genetically related to the geometry of large thrusts and their kinematic evolution (see Oncken, 1988, 1989). The rank pattern characteristic of the central Massif (data from Wolf, 1978) differs from the north by several aspects (Fig.8):

- Rank differences between strata of different age are absent or do not reflect a consistent pattern; thus, paleogeothermal gradients or the thickness of the former superimposition can not be reconstructed from rank gradients (further to the north, the data from the filling of the Mosel syncline give 40-50°C/km).
- The rank of the hangingwall of the Boppard thrust is considerably higher than that of the footwall (see Fig.8) and shows the tendency to increase towards the thrust (this effect however may be due to an equally increasing strain towards the thrust which is known to cause a strain-induced alignment of the aromate lamellae resulting in higher values for R_{max} and for the reflectance anisotropy, R_{max}-R_{min}, see Teischmüller *et al.*, 1979; Levine & Davis, 1984; Teichmüller, 1987).
- The rank of both, hangingwall and footwall sequence, is too high to be explained by burial during sedimentation, the thickness of post-Emsian sediments probably does not exceed 2-3 km (cf. Meyer & Stets, 1980; Oncken, 1984).
- Beneath the thrust an inverse rank gradient - with respect to stratigraphic age as well as to the stacked tectonic sequence - is effected which encompasses a thickness of roughly 1 km of the footwall (Fig.8).

The mentioned observations clearly point to strong overprinting of the prekinematic rank pattern by folding and tectonic stacking. However, the differences are not levelled out entirely.

The calculation of paleotemperatures meets with an essential difficulty: Since only strata of Emsian and possibly Siegenian age are present, and since the former thickness of the superimposing strata is neither known from analysis of rank gradients, nor from a neighbouring more complete succession, a time-temperature curve and thus the effective time of coalification can not be reliably constructed. Because of the obvious role of tectonic stacking in this region, the shape of the time-burial curve should rather resemble curve B in Fig.3. The problem is solved tentatively by taking a mean value between the well-known data from the northern Massif (t_{eff}: 45-60 Ma) and the southern Massif (t_{eff}: 15-30 Ma). The weakly constrained data thus only give a range for the temperatures reached during peak metamorphism: 220-270°C in the footwall with a slight increase towards the thrust, and 270-320°C in the hangingwall. Due to the synkinematically continuing coalification, the amount of thrust displacement derived from the temperature difference and the dip of the thrust plane with respect to the stratigraphic sequence is underestimated. The construction of balanced sections indicates 10-17 km for the Boppard thrust (the uncertainty due to lacking biostratigraphic data from the hangingwall) while the above mentioned differences only yield about half of this value.

Microfabric data again show a similar relationship with however more details (see also Fig.9). Quartz from early, pre- to syn-s_1-veins shows cold working and weak recovery features in the footwall (with continuous and discontinuous undulatory extinction, deformation bands, sutured grain boundaries, subgrains which may start to from high angle boundaries from progressive subgrain rotation). Quartz from the hangingwall is strongly recrystallised with development of a preferred crystallographic orientation and shape alignment, but without equilibrated grain boundaries. These features which point to synkinematic recrystallisation at peak temperatures during first cleavage formation are not found in later veins which are still deformed by s_1 or only by the second cleavage which is generally restricted to the hangingwall. Here, only cold-working and weak recovery features are developed (comp. to footwall) while a similar retrogressive sequence in the footwall is lacking. Within the central shear zone of the thrust, microfabrics characteristic of the hangingwall are lonly preserved in porphyroclasts which are deformed by cataclasis.

The phyllosilicate fabric shows similar trends: A penetrative alignment of sheet silicates develops parallel to s_1 with synkinematic growth to some 30 μm in the hangingwall compared to less

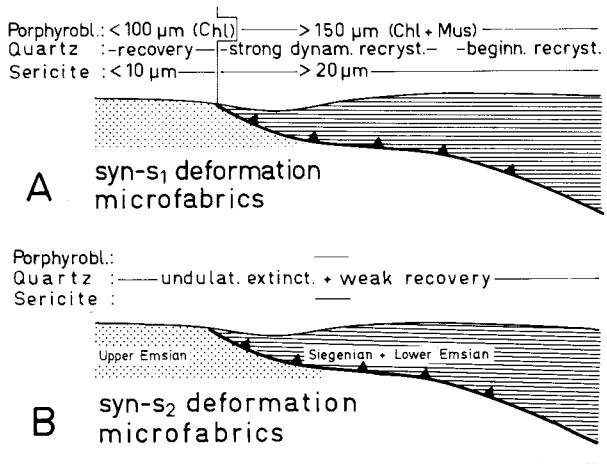

Fig.9.- Schematic distribution of fabric types and mineralisations across the Boppard thrust for first and second cleavage generations (Chl = Chlorite, Mus = Muscovite).

than 10 μm in the footwall. At the same time, sheet silicates are strongly polygonised only in the hangingwall. Similarly, the size of syn-s_1 chlorite and white mica porphyroblasts is considerably larger in the hangingwall than in the footwall. No such differences can be observed in the fabric of the second cleavage which shows merely kinking and bending of phyllosilicates and solution of quartz (preferentially at contact to 001 of phyllosilicates).

These observations on rank pattern and microfabric sequences show that thrust motion did not initiate before peak metamorphism which is found to be simultaneous to formation of the first cleavage (Weber, 1976). Thrusting then largely proceeds with transport of a «frozen» metamorphism of the hangingwall sequence under retrogressive conditions and progressive adjustment of conditions between the hangingwall and the footwall units. The development of this class of thrusts in the central Massif (schematically shown in Fig.10) involves the evolution of the hangingwall rocks along a retrogressive PT-path while the footwall sequence should show an unchanged or a slightly progressive PT-history (cf. Shi & Wang, 1987). The picture reflects rapid cooling of the hangingwall by the cooler footwall near the thrust, the upper part of the latter being heated up somewhat without however resulting in an inverse temperature gradient. The isothermes and the temperature gradients are merely subjected to some distortion along the thrust, since thermal relaxation will proceed faster than tectonic stacking (see similar models by Chamberlain & Karabinos, 1987; Shi & Wang, 1987). The inverse metamorphic gradient thus reflects different time spans during the deformation history of the hangingwall and footwall units and the metamorphic indicators can not be taken to give the deformation conditions of a simultaneous event.

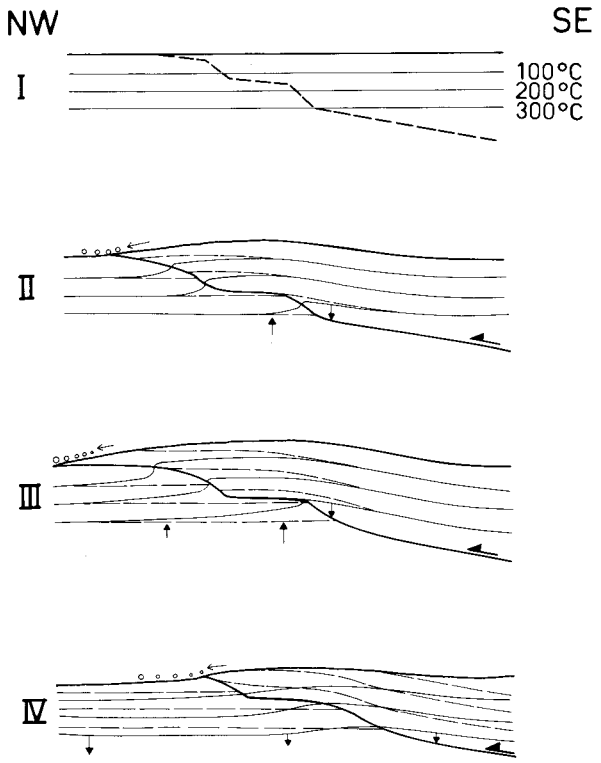

Fig.10.- Schematic illustration of motion of isothermes during thrusting for the thrust type of the central Massif with ramp-flat geometry; solid line shows actual, dashed line shows initial position of isothermes; arrows give directions of thrusting, erosion, and relative motion of isothermes; I: Initial stage before thrusting, II: early stage of thrusting (with beginning erosion fo hangingwall); III: main stage of thrusting; IV: after thrusting. The inverse gradient of metamorphism in stage IV is not paralleled by inverse paleogeothermal gradients, but is achieved by stacking and displacement of the pile through the isotherm field.

4.3.- The Taunskamm-nappe unit

The metamorphic conditions of the Taunuskamm thrust unit (Fig.11) at the southern border of the Rhenish Massif are well established from petrologic data by Meisl (1970, 1986), Meisl *et al.* (1982) and Massonne & Schreyer (1983). The association of pumpellyite + actinolite + chlorite + quartz west of the river Rhine gives between 320° at 2 kb or 300° at 4 kb to less than 360°C (see Winkler, 1979). East of the Rhine, the quartz-albite-muscovite-chlorite-facies reflects somewhat higher temperatures at lower greenschist conditions. Peak metamorphism is timed to be simultaneous to the deformation related to the dominating cleavage. Massonne & Schreyer (1983) and Meisl (1986) moreover determine confining pressures of 8-12 kb from phengite barometry which they take to reflect conditions of a subduction zone between the Rhenohercynian and the Saxothuringian zones. PT-conditions seem to decrease continuously towards the northwest (see also Oncken, 1988).

Microfabric features are well in accord with the above cited data. In the footwall below the Taunuskamm thrust, quartz shows well developed recovery features (discontinous undulatory extinction, deformation bands and lamellae, crystal plastic deformation by dislocation glide, strongly sutured grain boundaries). The ubiquitous subgrains may rotate progressively to give first high angle grain boundaries (synkinematic recrystallisation). Post-s_1-quartz-veins only show cold-working and weak recovery overprinted by cataclasis.

Independent from the stratigraphic position, the hangingwall sequence in addition shows increasing recrystallisation of quartz from west to east. Mylonites form by dynamic recrystallisation and acquire a preferred orientation of grain shape and crystallographic fabric. Grain boundaries may even, in some parts, equilibrate and show triple

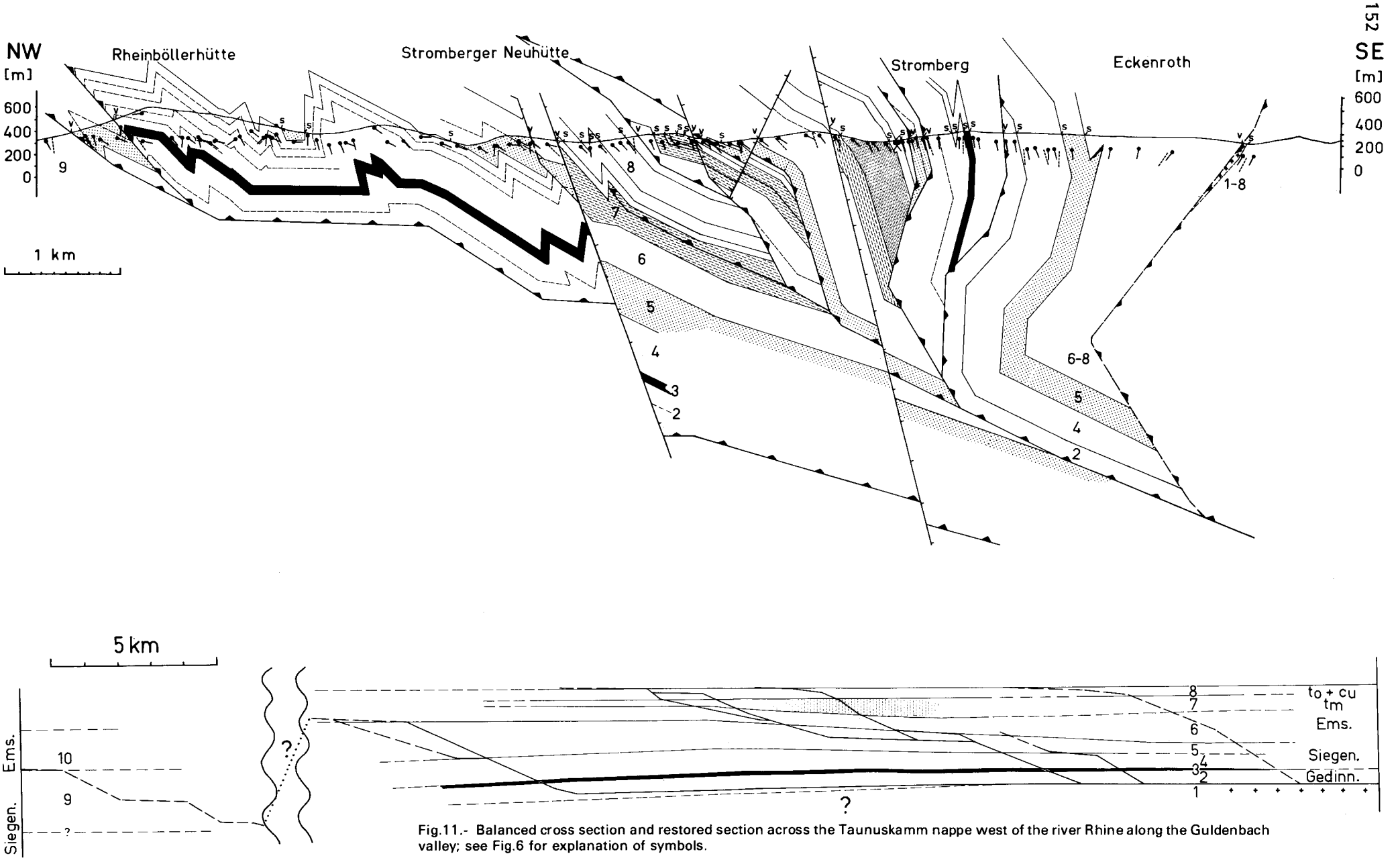

Fig.11.- Balanced cross section and restored section across the Taunuskamm nappe west of the river Rhine along the Guldenbach valley; see Fig.6 for explanation of symbols.

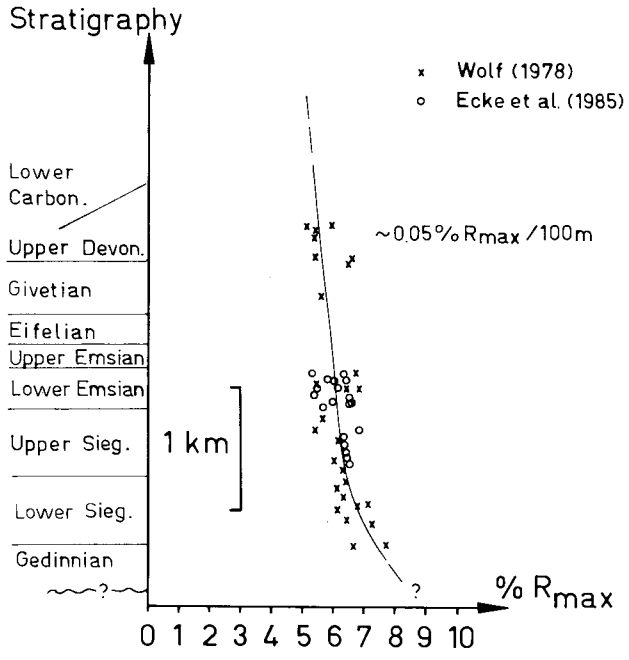

Fig.12.- Rank profile (vitrinite reflectance versus stratigraphic depth) for the Taunuskamm unit west of the river Rhine; source of rank data according to cited papers.

points and concave grain boundaries indicative of secondary grain growth driven by grain boundary energy. Calcite generally shows the same picture as quartz. These fabrics are overprinted by a later crenulation cleavage or by folding and cataclasis (in the shear zones). Instead of a general heating of the pile under static conditions, the mentioned annealing fabric is thought to reflect a progressive concentration of strain into the retrogressive shear zones at the base of the nappe pile. Post-s_1-quartz-veins only show cold working and weak recovery similar to the footwall.

The phyllosilicate fabric related to the dominating cleavage is polygonised in the hangingwall as well as in the footwall including considerable grain growth on the cleavage planes. Chlorite and white mica porphroblasts increase in size towards the southeast from 25-100 μm to 30-150 μm. However, the dominating cleavage fabric in pelitic strata from the hangingwall sequence generally is a second cleavage. The only rarely preserved first cleavage shows only minor grain growth and small chlorite porphyroblasts (< 25 μm). A third cleavage in these cases, just as the second in the footwall, crenulates the sheet silicates of the dominating older fabric, is not related to any formation of new grains, and only shows some solution of quartz. The whole sequence of cleavage fabrics thus records deformation under first progressive conditions followed by retrogressive conditions (see Oncken, 1988 for details).

The rank pattern differs from the northern and the central Massif (see Wolf, 1978 and Ecke *et al.*, 1985). Besides the lack of an apparent hiatus across the thrust zone, several facts are to be noted:

- No distinct rank gradient can be constructed from a rank profile (see Fig.12), the weak decrease of rank with stratigraphic age in the Stomberg syncline would yield an extremely high superposition while the thickness of the Devonian barely exceeds 3 km which is unable to explain the above mentioned PT-conditions.
- All strata show nearly the same rank of organic matter despite the large stratigraphic range; lines of equal rank seem to cut across the stratigraphic and tectonic stack.
- The average rank in some cases (< 5%R_{max}) does not reflect the conditions indicated by petrologic data.

A first conclusion to be drawn from these observations is the obvious role of synkinematic coalification which largely, but not entirely, obliterates pre-kinematic differences. Due to probably tectonic stacking, the whole imbricate stack of the nappe body must itself have been covered by another unit. At the same time, the heating time during stacking must have been short with respect to the reaction time of organic matter, since no equilibrium has been achieved.

Total burial and peak temperatures are not easily determined from rank data with the analytic tool presented, since the subsidence history after the Upper Devonian is not well defined. However, because of the knowledge of reached temperatures from petrologic data, the tool may be adapted to yield other parameters: A time-burial curve (better: a time-temperature curve) may be modelled which is able to explain the rank pattern; this curve moreover yields the approximate paleogeothermal gradients before deformation. Several additional data constrain the possible solution of the problem:

- Radiometric data (K/Ar) give an age of 325-330 Ma (see Ahrendt *et al.*, 1978) which seems to coincide with maximum subsidence and heating and which is simultaneous to deformation (through relationship between analysed mica grains and cleavage).
- The burial curves of the different stratigraphic units (from stratigraphic and thickness data) must converge during deformation before the mentioned time and rise together because of their identical synkinematic metamorphism (except for the minor differences in organic rank).
- Postkinematic sedimentation in the uppermost Carboniferous and the Rotliegend of the Saar-Nahe basin points, according to Kowalczyk (1983) and Lorenz & Nicholls (1984), to largely

accomplished uplift and erosion (because of relief and sediment type, detrital material corresponding to presently outcropping strata etc.).

Further assumptions include stable paleo-geothermal gradients during sedimentation followed by different, equally stable gradients during deformation.

These constraints allow the construction of time-temperature curves for different stratigraphic levels which meet the prerequesite of explaining the observed rank data. An essential consequence is the necessity of a minimum time span of tectonic stacking of > 2 Ma. Shorter periods are not able to nearly obliterate the rank differences between strata of different age and to effect a partly common level of organic metamorphism. Longer heating periods (> 20 Ma) on the other hand would compel a higher and uniform rank at the temperatures reached.

On the basis of the above mentioned constraints and of a temperature reached of 330-340°C model time-temperature curves for different stratigraphic levels have been constructed which fulfill the mentioned conditions (see Fig.13).

From the above temperature, from the organic rank (see Fig.12), and for a total subsidence time from start of sedimentation to the end of the Carboniferous the effective times of coalification for three stratigraphic levels are calculated (using Fig.2): 30 Ma for the Upper Gedinnian (7%R_{max}), 20 Ma for the Emsian (6%R_{max}), 15 Ma for the Givetian (4.8%R_{max}). These values are used to compute the variable x ($x = t_{eff}/t$; portion of the area above the curve in Fig.3) which then constrains the shape of the t-T-curve.

Assuming a stable paleo-geothermal gradient during sedimentation, the first part of the curves can be obtained from cumulative thickness data with a uniform 45°C/km for all three levels (higher or lower paleogeothermal gradients would fail to fulfill the above conditions). The model shows a subsequent phase of very rapid subsidence (< 5 Ma) due to tectonic stacking during the Lower Carboniferous. Uprise and erosion succeed equally rapid. The shape of the uprise part of the curve may be varied within a certain limit as long as the effective time of coalification remains unchanged. The depth reached during the phase of tectonic subsidence depends on the expected values for the

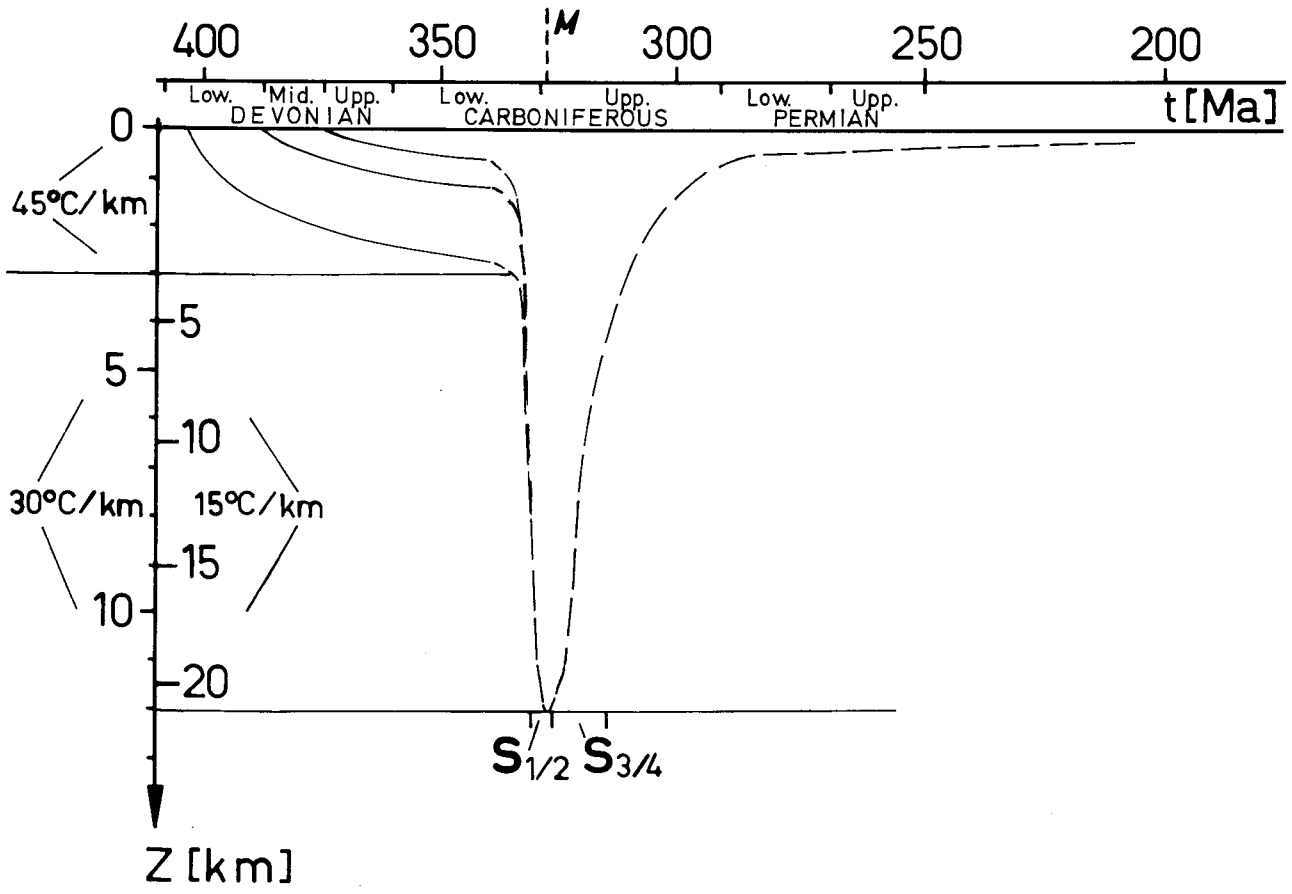

Fig.13.- Time-burial curves for three stratigraphic levels of the Taunuskamm unit at changing paleogeothermal gradients during burial and stacking. Time of peak metamorphism M (after Ahrendt *et al.* 1978), and cleavage generations in pelitic rocks are shown. Solid burial curves: subsidence constructed from data on cumulative sedimentary thickness; dashed lines: model curves satisfying the defined constraints (see text); time scale according to Haq & van Eysinga (1987).

paleo-geothermal gradients during stacking: A reasonable decrease from 45°C/km to 15-30°C/km resulting from stacking will yield 11-22 km (see Fig.13). This value ranges between Meisl's (1970) data from petrological observations (see also Meisl *et al.*, 1982) and the 24-32 km of Massonne & Schreyer (1983) and Meisl (1986). It appears that the latter data, obtained from phengite barometry which is calibrated experimentally under static conditions without taking into account the effects of synmetamorphic deformation and variations in fluid composition, may give exaggerated values. Also, these data pose the problem of the whereabouts of the former superimposition and its original paleogeographic position.

The weak coalification drop at the sole thrust of the Taunuskamm nappe (from 5-7% in the hangingwall to 5-6%R_{max} in the footwall) yield a throw of 1 km at the most. However, the primary difference has obviously been affected by synkinematic heating of the pile. In contrast to parts of the northern and central Massif, differences in organic rank thus can not be used to infer thrust displacement and throw in the southern Massif. At most, the slight decrease of synkinematic temperatures from southeast to northwest at the present erosional level is subjected to a minor drop beneath ca. 300°C.

Moreover, figure 13 illustrates another aspect of the deformation history. Deformation under prograde PT-conditions with the peak of penetrative deformation proceeds very rapidly during tectonic stacking: Data on the strain of the thrust body (shortened to a third of its former length), on the end of sedimentation, and on the time of metamorphism yield a mean strain rate of the thrust body of approximately $10^{-14}s^{-1}$. This value agrees with the data compiled by Pfiffner & Ramsay (1982). The strain rate within the shear zones is expected to be higher by one or two orders of magnitude. The strain rate during the weaker deformation under retrogressive conditions is considerably lower.

All data thus give a relatively consistent picture of the deformation-temperature history:

- Deformation and imbrication of the thin Devonian sequence occur during tectonic stacking under progressive metamorphic conditions up to temperatures which allow the dynamic recrystallisation of quartz, calcite and the polygonisation of sheet silicates (at some 300°C).
- Subsequent deformation proceeds under retrogressive conditions during uplift and erosion below the temperature limit for recovery of the mentioned minerals with a final stage of brittle fracture, and appears to be concentrated to the shear zones (see Oncken, 1988).

The entire process thus is not related to the transport of a frozen metamorphism, but instead - differing from the central Massif - is connected to a synkinematic metamorphic overprinting of the evolving structure during overriding of superincumbent nappes in a continental collision environment.

5.- DISCUSSION AND CONCLUSION

A number of papers group large parts of the Rhenish Massif (i.e. of the presently outcropping surface) into the very low grade metamorphic zone of the prehnite-pumpellyite-quartz-facies sensu Winkler (1979; see Meisl, 1970, 1986; Weber, 1972, 1976; Koschinski, 1979; Teichmüller *et al.*, 1979; Weber & Behr, 1983). Except from parts of the northern Massif and the Eifel synclinorium, paleotemperatures range between 200 and 350°C at 1-3 kbars (the Venn anticline shows still higher temperatures, Kramm, 1982). Similar to the other parts of the Variscan orogen, the Rhenish Massif is thus characterised by a high-T, low P-metamorphism with high prekinematic paleo-geothermal gradients (see Teichmüller *et al.*, 1979; Buntebarth, 1982; Oncken, 1984, 1987) from 30-80°C/km in the north and ranging at 45°C/km in the south. In contrast, the southern boundary of the Massif shows, along a narrow zone, similar or somewhat higher temperatures (300-400°C) reaching low grade conditions with high pressures and low synkinematic paleo-geothermal gradients (see Meisl, 1970, 1986; Meisl *et al.*, 1982; Massonne & Schreyer, 1983).

Generally, the peak temperatures during metamorphism coincide, following observations on cleavage fabrics (Weber, 1976) and K/Ar-ages of mica crystallisation (Ahrendt *et al.*, 1978), with the dominant cleavage (usually s_1) and peak deformation. In parts of the northern Massif, lines of equal rank parallel the folded sedimentary sequence (Paproth & Wolf, 1973) and thus point to largely prekinematic coalification with little change during deformation. In the rest of the Massif, this relationship is not observed due to the stronger effect of a synkinematic thermal overprinting. The later deformation phases (s_2 or s_3) develop during retrogressive uplift (see Weber, 1976; Meisl *et al.*, 1982; Oncken, 1988).

These observations agree well with the analysis of the regional pattern of published rank data and of the pattern of deformation fabrics and mechanisms of some principal rock-forming minerals: Within the Eifel synclinorium and north of the Ennepe-fault at the northern border of the

Rhenish Massif, the only fabric present are cold working structures (undulatory extinction in quartz, twinning in calcite, kinking of sheet silicates) cataclasic deformation, and some solution of calcite. South of the Ennepe-fault, at temperatures rising above 200°, small chlorite cross mica and authigenous albite appear (together with solution of quartz and quartz-/chlorite-veins).

Further south, in the cores of the large anticlines (Remscheid, Ebbe) higher thermal conditions are realised (recovery fabrics in quartz, beginning recrystallisation of quartz at the appearance of paragonite and pyrophyllite, larger chlorite cross mica and smaller muscovite cross mica synkinematic to s_1). Abundant formation of chlorite and solution of quartz accompanied by widespread synkinematic formation of quartz-/chlorite-filled shear and extension veins in cataclasites and neighbouring areas point, besides the increasing role of diffusional processes, to exaggerated pore fluid pressures during especially the first part of the deformation history. The final part of the deformation history shows none of the recorded fabrics and only includes brittle fracture with weak mineralisation.

Quartz in syn-s_1-veins in hangingwalls of larger thrusts of the southern Massif generally was subjected to pervasive dynamic recrystallisation which may increase towards the southeast (at the same time: recovery fabrics in quartz, calcite, and sheet silicates; chlorite and white mica prophyroblasts). Within the footwalls of large thrust systems, this inventory decreases rapidly in importance with increasing distance from the thrusts towards the northwest (resulting in the formation of inverse metamorphic gradients which, however, reflect an older, transported metamorphism of the hangingwalls). «Warm» fabrics within shear zone rocks are moreover only preserved within porphyroclasts which in their turn are strongly affected by fracture and solution. Conditions of subsequent retrogressive deformation do not differ across the thrusts. Furthermore this drop of PT-conditions below the temperature threshold for the onset of recovery mechanisms in quartz (< 200°) is supported by the stability of dickite (needing > 100°, see Kübler *et al.*, 1979, and less than the temperature for the pyrophyllite transition) suggesting a reduction of the thickness of the thrust bodies to less than half of their original thickness during final motion. This part of the Massif shows predominant crystal plastic deformation mechanisms with abundant diffusion controlled mechanisms (pressure solution and grain boundary diffusion), the latter increasing in importance during deformation and related grain-size reduction, both being succeeded by cataclastic deformation.

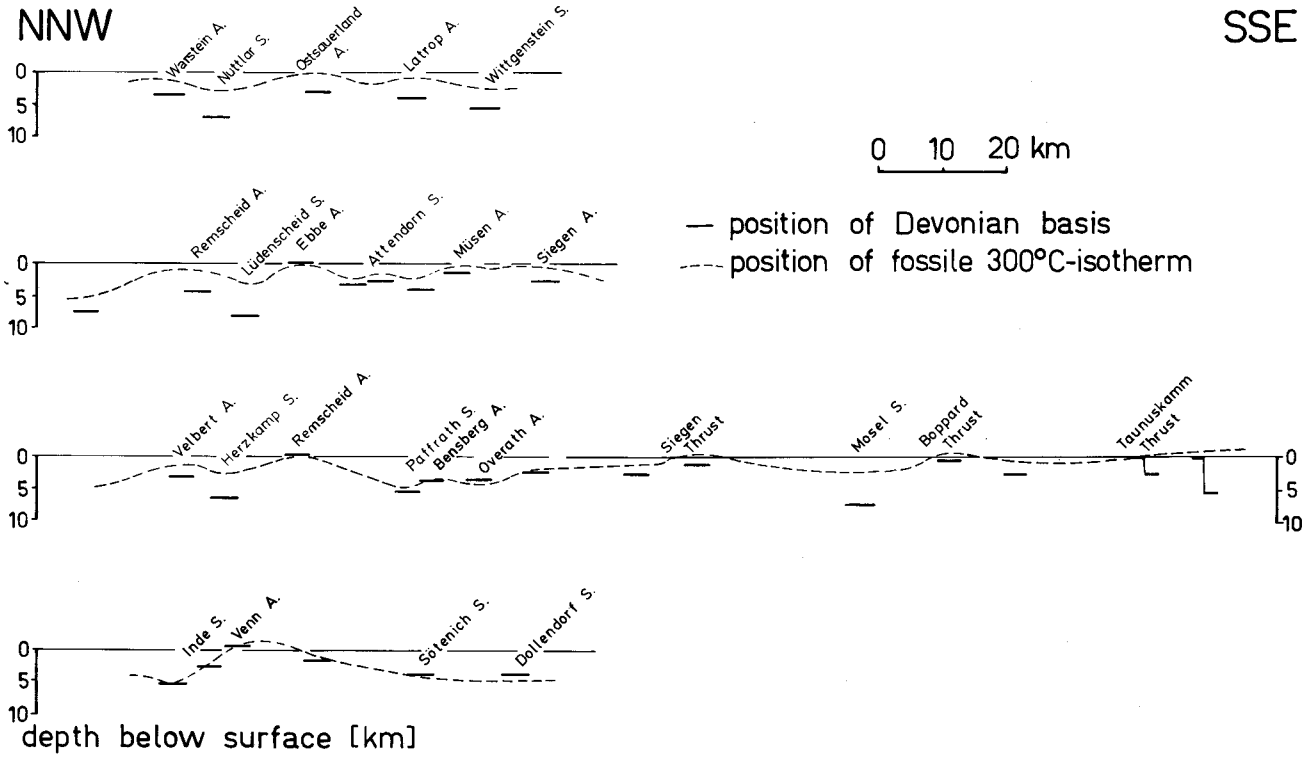

Fig.14.- Former relationship between 300°C-isotherm and position of Devonian basis during Variscan deformation; the position of the first is determined from rank analysis, the latter is determined from outcrop data and the evolution of rates of sedimentation and thicknesses (see Oncken, 1987); names refer to major anticlines (A), synclines (S) and thrusts; the sections range from the eastern (top) to the western (bottom) Rhenish Massif with the long section paralleling the Rhine valley.

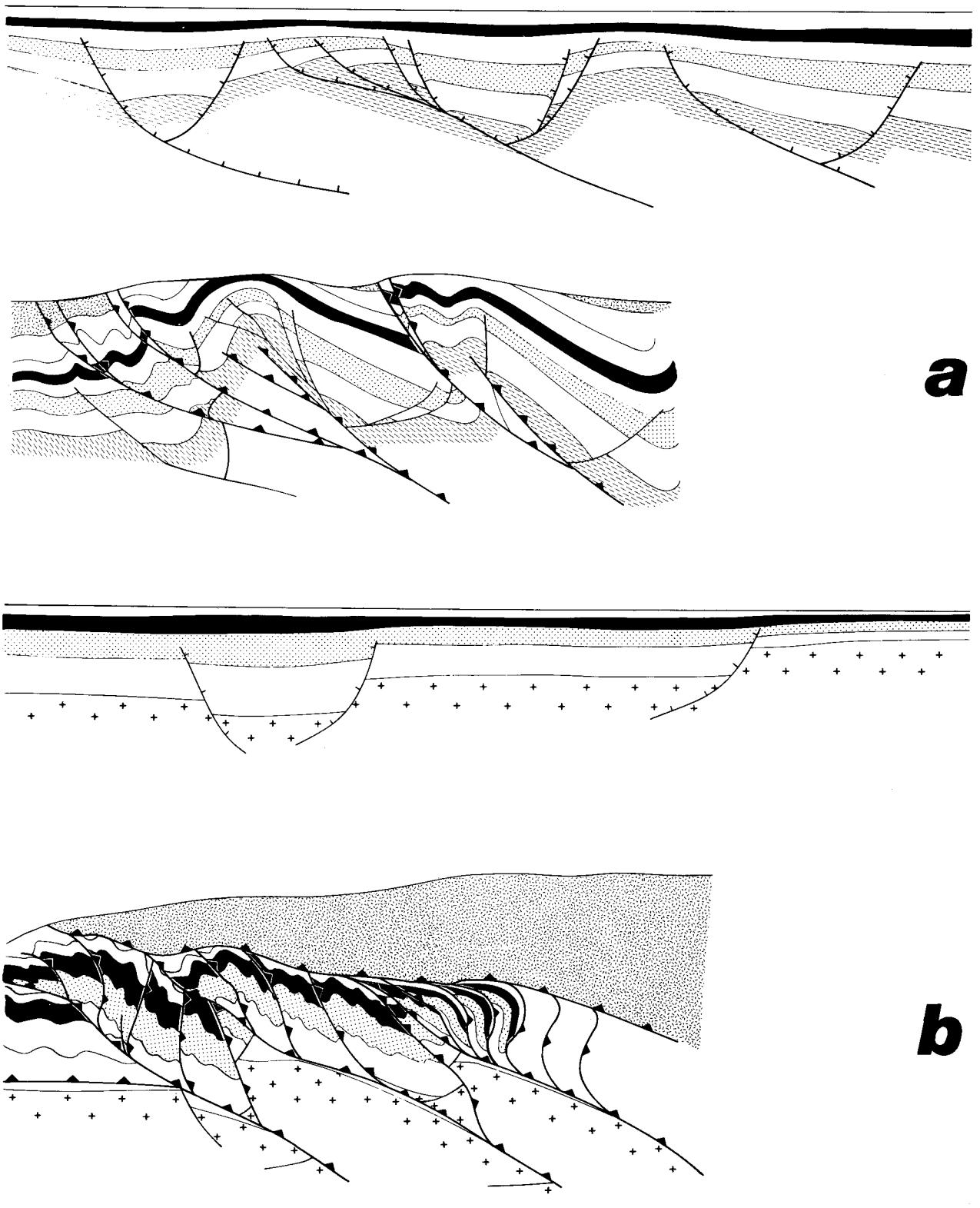

Fig.15.- Schematic structural evolution from late basin stage to late stage of deformation; a) structural type of northern Massif, b) structural type of central and southern Massif.

The metamorphism of the Taunuskamm nappe body and the Boppard thrust body, moreover, can not be explained by the thickness of the sedimentary cover or by synkinematically increasing paleo-geothermal gradients. Besides the observation that lines of equal rank cut across the imbricated sequence, a larger tectonic superposition due to stacking is required for most of the southern Massif. It thus appears probable, that the nappe body of the «Gießen Grauwacke» (see Kossmat, 1931, Engel *et al.,* 1983) has formerly had a much larger extension than its present remains would suggest.

On the whole, the analysis leads to a picture of narrow zones along strike of equal metamorphism which are separated by thrusts from each other while the degree of metamorphism shows a general tendency to increase towards the southeast in discrete steps. The schematic illustration of this aspect in figure 14 moreover yields another relationship: The 300°-paleo-isotherm roughly follows the basis of the Devonian basin filling; below thrusts, the isotherm is uplifted due to synkinematic heating during stacking; from west to east, the mentioned isotherm rises with respect to the Devonian basis - possibly a hint to an increasing influence of tectonic stacking during deformation in the same direction and/or of higher paleogeothermal gradients (cf. Teichmüller *et al.,* 1979; Weber & Behr, 1983).

Similarly, these zones correlate to changes in relevant deformation mechanisms which is also emphasised by the observation of the regional pattern of deformation microfabrics (see above). The difference in tectonic styles of the northern and southern Massif (large scale folds with associated reverse faults, both controlled by the geometry of the basin filling versus penetrative cleavage and pervasive imbricating controlled by the geometry of the basement; see Fig.15) obviously is strongly influenced by this zoning of thermally activated deformation mechanisms along the present outcrop: The presently exposed surface thus represents an oblique horizontal section through the post-Variscan crust descending through different former structural levels with different thermal regimes and dominating deformation mechanisms towards the southeastern suture between the Rhenohercynian and Saxothuringian zones.

BIBLIOGRAPHY

AHRENDT, H., HUNZIKER, J. & WEBER, K., 1978. K/Ar-Altersbestimmungen an schwach metamorphen Gesteinen des Rheinischen Schiefergebirges. - *Z. dt. geol. Ges.* 129: 229-247, Hannover.

BOSTICK, N.H., 1973. Time as a factor in thermal metamorphism of phytoclasts. - *In:* 7ème Congr. Int. de Stratigr. et de Géol. du Carbonifère, Krefeld. Compte rendu 2: 183-192.

BOSTICK, N.H., CASHMAN, S.M., Mc CULLOH, T.H. & WADELL, C.T., 1979. Gradients of vitrinite reflectance and present temperature in the Los Angeles and Ventura basins, California. - *In:* Low temperature metamorphism of kerogen and clay minerals (ed.: D.F. Oltz); *Pacific Section, Soc. Econ. Paleont. Miner.* 65-96.

BREITSCHMID, A., 1982. Diagenese und schwacke Metamorphose in den sedimentären Abfolgen der Zentralschweizer Alpen (Vierwaldstätter See, Urirotstock). - *Eclogae geol. Helv.* 75/2: 331-380.

BUNTEBARTH, G., 1979. Eine empirische Methode zur Berechnung von paläogeothermischen Gradienten aus dem Inkohlungsgrad organischer Einlagen in Sedimentgesteinen mit Anwendung auf den mittleren Oberrhein-Graben. Krefeld - *Fortschr. Geol. Rheinld. u. Westf.* 27: 97-108.

CHAMBERLAIN, C.P. & KARABINOS, P., 1987. Influence of deformation on pressure-temperature paths of metamorphism. - *Geology,* 15: 42-44.

ECKE, H.H., HOFFMANN, M., LUDEWIG, B. & RIEGEL, W., 1985. Ein Inkohlungsprofil durch den südlichen Hunsrück (südwestliches Rheinisches Schiefergebirge). Stuttgart. *N. Jb. Geol. Paläont. Mh.* 1985/7: 395-410.

ENGEL, W., FRANKE, W., GROTE, C., WEBER, K., AHRENDT, H. & EDER, F.W., 1983. Nappe Tectonics in the Southeastern Part of the Rheinisches Schiefergebirge. - *In:* (eds.: H. Martin & F.W. Eder) Intracontinental Fold Belts - Case Studies in the Variscan Belt of Europe and the Damara Belt of Namibia. 267-287, (Springer) Berlin/Heidelberg/New York/Tokyo.

FREY, M., 1987. Low Temperature Metamorphism. - 351 p., (Blackie) Glasgow and London; (Chapman & Hall) New York.

FREY, M. & NIGGLI, E., 1971. Illitkristallinität, Mineralfazies und Inkohlungsgrad. - *Schweiz. mineral. petrol. Mitt.* 51: 229-234.

FREY., M., TEICHMUELLER, M., TEICHMUELLER, R., MULLIS, J., KUENZI, B., BREITSCHMID, A., GRUNER, U. & SCHWIZER, B., 1980. Very low-grade metamorphism in external parts of the Central Alps: Illite crystallinity, coal rank, and fluid inclusion data. *Eclogae geol. Helv.* 73/1: 173-203.

HAQ, B.U. & VAN EYSINGA, F.W.B., 1987. Geological Time Table. (Elsevier) Amsterdam.

HOOD, A., GUTJAHR, C.C.M. & HEACOCK, R.L., 1975. Organic Metamorphism and the Generation of Petroleum. *Am. Ass. Petr. Geol. Bull.* 59: 986-996.

KARWEIL, J., 1955. Die Metamorphose der Kohlen vom Standpunkt der physikalischen Chemie. *Z. dt. geol. Ges.* 107: 132-139.

KARWEIL, J., 1973. The determination of paleotemperatures from the optical reflectance of coaly particles in sediments. - *In:* B. Alpern (ed.): Colloque international sur la pétrographie et la matière organique des sédiments, relations avec la paléotemperature et le potentiel pétrolier. C.N.R.S., Paris. 196-203.

KERRICH, R., BECKINSALE, R.D. & DURHAM, J.J., 1977. The transition between deformation regimes dominated by intercrystalline diffusion and intracrystalline creep evaluated by oxygen isotope thermometry. *Tectonophysics,* 38: 241-257.

KISCH, H.J., 1980. Illite crystallinity and coal rank associated with lowest grade metamorphism of the Taveyanne greywacke in the Helvetic zone of the Swiss Alps. Basel. *Eclogae geol. Helv.* 73/3: 753-777.

KNIPE, R.J., 1981. The interaction of deformation and metamorphism in slates. *Tectonophysics,* 78: 249-272.

KOSCHINSKI, G., 1979. Mikrostrukturelle und mikrothermometrische Untersuchungen an Quarzmineralisation aus dem östlichen Schiefergebirge. Göttingen. *Diss. Univ. Göttingen,* 156 p.

KOSSMAT, F., 1931. Das Problem der Großüberschiebungen im variskischen Gebirge Deutschlands. *Centralbl. f. Min. etc., Abt. B.,* 11: 577-602.

KOWALCZYK, G., 1983. Das Rotliegende zwischen Taunus und Spessart. *Geol. Abh. Hess.* 84: 1-99.

KRAMM, U., 1982. Die Metamorphose des Venn-Stavelot-Massivs, nordwestliches Rheinisches Schiefergebirge: Grad, Alter und Ursache. *Decheniana,* 135: 121-178.

KUEBLER, B., PITTION, J.L., HEROUX, Y., CHAROLLAIS, J. & WEIDMANN, M., 1979. Sur le pouvoir réflecteur de la vitrinite dans quelques roches du Jura, de la molasse et des Nappes Préalpines Helvétiques et Penniniques (Suisse occidentale et haute Savoie). *Eclogae geol. Helv.* 72/2: 347-373.

LEVINE, J.R. & DAVIS, A., 1984. Optical anisotropy of coals as an indicator of tectonic deformation, Broad Top Coal Field, Pennsylvania. *Geol. Soc. Amer. Bull.* 95: 100-108.

LORENZ, V. & NICHOLLS, I.A., 1984. Plate and microplate Processes of Hercynian Europe during the Late Paleozoic. *Tectonophysics,* 107: 25-56.

MASSONE, H.J. & SCHREYER, W., 1983. A new experimental phengite barometer and its application to a Variscan subduction zone at the soutern margin of the Rhenohercynicum. *Terra Cognita,* 3: 187.

MEISL, St., 1970. Petrologische Studien im Grenzbereich Diagenese-Metamorphose. *Abh. hess. L.-A.f.* Bodenforsch. 57: 1-93.

MEISL, St., 1986. Mineralogisch-petrographische Exkursion in den Soonwald - DMG-Tagung, 1986 Exkursion A2. *Fortschr. Miner.* 64/2: 35-95.

MEISL, St., ANDERLE, H.J. & STRECKER, G., 1982. Niedrigtemperierte Metamorphose im Taunus und im Soonwald - DMG-Tagung, 1982 Exkursion E3. *Fortschr. Miner.* 60/2: 43-69.

MEYER, W. & STETS, J., 1980. Zur Paläogeographie von Unter- und Mitteldevon im westlichen Schiefergebirge. *Z. dt. geol. Ges.* 131: 725-751.

MITRA, Sh., 1987. Regional variations in deformation mechanisms and structural styles in the central Appalachian orogenic belt. *Geol. Soc. Amer. Bull.* 98: 569-590.

NICOLAS, A. & POIRIER, J.P., 1976. Crystalline Plasticity and Solid State Flow in Metamorphic Rocks. (J. Wiley) London/New York/Sydney/Toronto. 444 p.

ONCKEN, O., 1984. Zusammenhänge in der Strukturgenese des Rheinischen Schiefergebirges. *Geol. Rdsch.* 73: 619-649.

ONCKEN, O., 1987. Heat Flow and Kinematics of the Rhenish Basin. - *In:* (eds.: A Vogels, H. Miller & R. Greiling). The Rhenish Massif, (Vieweg, Earth Evolution Series) Braunschweig. 63-78.

ONCKEN, O., 1988. Geometrie und Kinematik der Taunuskammüberschiebung - Beitrag zur Diskussion des Deckenproblems im südlichen Schiefergebirge. *Geol. Rdsch.* 77: 551-575.

ONCKEN, O., 1989. Geometrie. Deformationsmechanismen und Kinematik großer Störungszonen der hohen Kruste (Beispiel Rheinisches Schiefergebirge). *Geotektonische Forschungen* (in press).

PAPROTH, E. & WOLF, M. 1973. Zur paläogeographischen Deutung der Inkohlung im Devon und Karbon des nördlichen Rheinischen Schiefergebirges. *N. Jb. Geol. Paläont. Mh.* 1973: 469-493.

PFIFFNER, O.A. & RAMSAY, J.G., 1982. Constraints on Geological Stain Rates: Arguments from Finite Strain States of Naturally deformed Rocks. *J. Geophys. Res.* 87: 311-321.

SHI, Y. & WANG, C.-Y., 1987. Two-dimensional modeling of the P-T-t-paths of regional metamorphism in simple overthrust terranes. *Geology,* 15: 1048-1051.

STACH, E., MACKOWSKY, M-Th., TEICHMUELLER, M., TAYLOR, G.H., CHANDRA, D. & TEICHMUELLER, R., 1975. Stach's Textbook of Coal Petrology. - 2nd ed., (Borntraeger) Berlin Stuttgart. 428 p.

TEICHMUELLER, M., 1987. Recent advances in coalification studies and their application to geology. - *In:* Coal and Coal-bearing Strata: Recent Advances (ed.: A.C. Scott), *(Geol. Soc. Spec. Publ.* 32: 127-169.

TEICHMUELLER, M., 1987. Organic material and very low-grade metamorphism. - *In:* Low Temperature Metamorphism (ed.: M. Frey), 141-161, (Blackie) Glasgow and London, (Chapman & Hall) New York.

TEICHMUELLER, M., TEICHMUELLER, R. & WEBER, K., 1979. Inkohlung und Illitkristallinität. Vergleichende Untersuchungen im Mesozoikum und Paläozoikum von Westfalen. *Fortschr. Geol. Rheinld. u. Westf.* 27: 201-276.

TISSOT, B.P., PELET, R. & UNGERER, Ph., 1987. Thermal history of sedimentary basins, maturation indices, and kinetics of oil and gas generation. *Am. Ass. Petr. Geol. Bull.* 71: 1445-1466.

VERNON, R.H., 1983. Metamorphic Proceses. Reactions and Microstructure Development. 247 p., (Allen & Unwin) London.

VOLL, G., 1976. Recrystallisation of quartz, biotite, and feldspars from Erstfeld to the Leventina Nappe, Swiss Alps, and its geological significance. *Schweiz. mineral. petrol. Mitt.* 56: 641-647.

WAPLES, D.W., 1980. Time and Temperature in Petroleum Formation: Application of Lopatin's Method to Petroleum Exploration. *Am. Ass. Petr. Geol. Bull.* 64: 916-926.

WEBER, K., 1972. Kristallinität des Illits und andere Kriterien schwacher Metamorphose im nordöstlichen Schiefergebirge. *N. Jb. Geol. Paläont. Abh.* 141: 333-363.

WEBER, K., 1976. Gefügeuntersuchungen an transversalgeschieferten Gesteinen aus dem östlichen Rheinischen Schiefergebirge. *Geol. Jb.* 94, Reihe D 15: 98 p.

WEBER, K. & BEHR, H.J., 1983. Geodynamic Interpretation of the Mid-European Variscides. - *In:* (eds.: H. Martin & F.W. Eder) Intracontinental Fold Belts. Case Studies in the Variscan Belt of Europe and the Damara Belt in Namibia, (Springer) Berlin/Heidelberg/New York/Tokyo. 427-469.

WHITE, S., 1976. The effects of strain on the microstructures, fabrics, and deformation mechanisms in quartzites. *Phil. Trans. R. Soc. Lond.* A 283: 69-86.

WHITE, S.H. & KNIPE, R.J., 1978. Microstructure and cleavage development in selected slates. *Contrib. Mineral. Petrol.* 66: 165-174.

WINKLER, H.G., 1979. Petrogenesis of Metamorphic Rocks. - 5th. ed., 348 p. (Springer) New York/Heidelberg/Berlin.

WOLF, M., 1972. Beziehungen zwischen Inkohlung und Geotektonik im nördlichen Rheinischen Schiefergebirge. *N. Jb. Geol. Paläont. Abh.* 141: 222-257.

WOLF, M., 1975. Ueber die Beziehungen zwischen Illit-Kristallinität und Inkohlung *N. Jb. Geol. Paläont. Mh.* 1975: 437-447.

WOLF, M., 1978. Inkohlungsuntersuchungen im Hunsrück (Rheinisches Schiefergebirge). *Z. dt. geol. Ges.* 129: 217-227.

WOOD, D., 1988. Relationships between thermal maturity indices calculated using Arrhenius Equation and Lopatin Method: Implications for Petroleum Exploration. *Am. Ass. Petr. Geol. Bull.* 72: 115-135.